

Flux syntheses of La-doped NaTaO₃ and its photocatalytic activity

Digamber G. Porob, Paul A. Maggard*

Department of Chemistry, North Carolina State University, Raleigh, NC 27695-8204, USA

Received 17 January 2006; received in revised form 12 March 2006; accepted 14 March 2006

Available online 18 March 2006

Abstract

The La-doped (2%) NaTaO₃ perovskite-type solid was synthesized in high purity and homogeneity within a molten Na₂SO₄/K₂SO₄ (1:1 molar ratio) flux in much shortened reaction times, 0.5–1.0 h, compared to conventional solid-state techniques. The particle morphologies were investigated by scanning electron microscopy and were irregular block-shaped with dimensions of 500–100 nm and smaller surface features. The bulk particle sizes were found to decrease with increasing amounts of flux used in the synthesis, from 1:1 (NaTaO₃:flux), 1:2 to 1:3 for a reaction duration of 1 h. Photocatalytic activities of the NaTaO₃ products were measured in an aqueous methanol solution to be 535–1115 μmol H₂ h⁻¹ g⁻¹, and which increased with increasing particle sizes and decreasing amounts of flux used in the synthesis. These rates were up to × 2 greater than that measured for a conventionally prepared La-doped (2%) NaTaO₃ sample, which is currently one of the most efficient UV-photocatalysts known.

© 2006 Elsevier Inc. All rights reserved.

Keywords: Sodium tantalate (NaTaO₃); Flux synthesis; Photocatalysis

1. Introduction

Many recently discovered photocatalytic systems based on early transition-metal oxides exhibit high (>10%) quantum efficiencies for the absorption of ultraviolet light and production of H₂ and/or O₂ from aqueous solutions [1–3]. An increasing number of examples have demonstrated that surface morphology/microstructure as well as particle size are significant factors in their photocatalytic activities, such as found for Bi₂WO₆ in the form of nanoplates [4], accessible interlayer spaces such as in the layered perovskites K₂La₂Ti₃O₁₀ and RbPb₂Nb₃O₁₀ [5–7], and the tunnel structures of BaTi₄O₉ or Na₂Ti₆O₁₃ [8,9]. Among the most active photocatalysts, 2% La-doped Sodium tantalate (NaTaO₃) currently exhibits the highest quantum efficiency (~56% at 270 nm) [10,11]. Its high activity has been attributed, via electron microscope observations, to ordered surface nanostep structures on particles that are 100–700 nm and that are attributed specifically to lanthanum doping into the structure. For comparison, nondoped NaTaO₃ particles with sizes of

2–3 μm and flat surfaces exhibit decreased rates by a factor of four times or more [10,11]. The nanostep surfaces of La-doped NaTaO₃ create both a higher surface area as well as separate surface sites for H₂/O₂ production and inhibit recombination. These results have recently been repeated and confirmed with the doping of the alkaline-earth cations Ca, Sr, and Ba into NaTaO₃, and which revealed a relationship between the size of the dopant and the surface nanosteps and particle sizes [12]. Thus, investigations into new synthetic preparations that result in more controlled particle sizes and morphologies are important in the study of efficient photocatalyst systems.

While La-doped NaTaO₃ has been intensely researched for the surface features that lead to its high activity, almost all of the photocatalytic studies of La-doped NaTaO₃ have been based on solid-state synthetic procedures that provide relatively limited or no control over particle sizes or morphologies. A few relevant studies include the synthesis of non-doped NaTaO₃ by low-temperature hydrothermal or solvothermal methods [13,14], but for which it is unknown whether La-doping is possible by these procedures or if these would lead to improvements in the photocatalytic rates. By contrast, molten salt (or flux) synthetic methods have shown the ability to accelerate the

*Corresponding author. Fax: +1 919 515 5079.

E-mail address: Paul_Maggard@ncsu.edu (P.A. Maggard).

relatively slow diffusion of reactants and to control the crystal growth of metal oxides particles, such as found for $RTaO_4$ ($R = \text{Gd, Y, Lu}$) [15], $Bi_4Ti_3O_{12}$ [16], Bi_2WO_6 [17] and $PbNb_2O_6$ [18] using as fluxes mixtures of Na_2SO_4/K_2SO_4 , $NaCl/KCl$ or Na_2SO_4/Li_2SO_4 . Further, particles with anisotropic and textured microstructures and controlled particle sizes can be obtained, such as we recently reported in the flux syntheses of the layered $Bi_5Ti_3FeO_{15}$ and $LaBi_4Ti_3FeO_{15}$ Aurivillius phases [19]. Thus, molten-salt flux methods are suitable for probing the effects that particle morphologies, sizes, and surface features, have on their photocatalytic activity, and which would lead to new insights regarding the origins of their photocatalytic activities.

Reported herein is the flux syntheses of La-doped (2%) $NaTaO_3$ and an investigation of its photocatalytic activity compared to the products obtained from the known solid-state methods. The synthetic conditions varied included the reactant-to-flux ratio and the reaction duration, both of which control the resultant particle sizes. The products were characterized by powder X-ray diffraction (PXRD), UV-Vis diffuse reflectance spectroscopy, and scanning electron microscopy (SEM). Measurements of their photocatalytic activities were performed in an aqueous methanol solution, both in order to evaluate the effects of the particles sizes and morphologies obtained by different flux reactions as well as for comparison to the products obtained by solid-state methods.

2. Experimental

2.1. Synthesis and characterization

A series of La-doped (2%) $NaTaO_3$ compounds were synthesized from a stoichiometric mixture of AR grade Na_2CO_3 , Ta_2O_5 and La_2O_3 (preheated at 850°C) using a Na_2SO_4/K_2SO_4 (1:1 molar ratio) flux. The reactants were ground together using a mortar and pestle and then combined with the Na_2SO_4/K_2SO_4 salts at different $NaTaO_3$:flux ratios from 1:1 to 1:4.8. The reactant mixtures were placed inside an alumina crucible and heated at 900°C for 0.5–1 h. Finally, the resulting products were washed with hot deionized water several times to remove the alkali metal salts. A fine homogeneous white powder of La-doped $NaTaO_3$ was obtained in high purity, as judged from PXRD data. The solid-state preparation of La-doped $NaTaO_3$ followed the reported procedures [10]. High-resolution PXRD pattern of all products were collected on an INEL diffractometer using $CuK\alpha_1$ ($\lambda = 1.54056 \text{ \AA}$) radiation from a sealed-tube X-ray generator (35 kV, 30 mA) in transmission mode using a curved position sensitive detector (CPS120). SEM on a JEOL JEM 6300 was performed to examine the particle microstructures and approximate sizes of the reaction products, and energy dispersive X-ray (EDX) analyzes were used to verify the approximate elemental compositions. In order to measure the band gaps and study the effect of particle size on the

reflectance characteristics of all samples, UV-Vis diffuse reflectance spectra (DRS) were collected on a CARY 3E spectrophotometer equipped with an integrating sphere.

2.2. Photocatalysis testing

Photocatalytic testing was conducted using an outer-irradiation-type quartz reaction cell with a volume of 180 mL, and which was illuminated through an 80 mm diameter window that was fitted and sized to the output window of a 400 W Xe arc-lamp. Each sample was first loaded with platinum (1 or 2 wt%), a well-known kinetic aid for the reduction of H_2O at the surfaces to give H_2 , by the photodeposition method as reported [10]. ~ 200 mg of $NaTaO_3$ was suspended via a magnetic stir bar in 180 mL of an aqueous solution of dihydrogen hexachloroplatinate(IV) ($H_2PtCl_6 \cdot 6H_2O$; Alfa Aesar, 99.95%), and that was then irradiated for 2 h using the 400 W Xe arc-lamp. After platinization, the resulting solution was filtered and dried to give a grayish-colored product. Next, a 20% aqueous methanol solution was used to fill the quartz reaction cell and a weighed (200 mg) amount of the platinized $NaTaO_3$ was added. The filled reaction cell was connected to a closed gas line that trapped the evolved gases inside an inverted graduated cylinder. This suspension was stirred continuously under irradiation with full solar spectrum light (200–>1000 nm) using a 400 W Xe arc-lamp equipped with a water heat filter to remove infrared radiation. During the course of the photocatalytic reactions, copious amounts of large bubbles continued to rise to the top of the reaction cell. Measurements of the rates of the photocatalytic reactions were taken volumetrically every hour and used to calculate the amount of gases generated (the sealed vessel preventing any losses from evaporation). Identity of the formed gases and their molar ratios were characterized via injection into a GC (SRI MG #2, helium ionization and thermal conductivity detectors).

3. Results and discussion

The PXRD patterns of the 2% La-doped $NaTaO_3$ flux products are shown in Figs. 1b–g, for reaction times of 0.5 and 1.0 h and product:flux molar ratios of 1:1, 1:2 and 1:3. For comparison, the PXRD pattern of the solid-state preparation of La-doped $NaTaO_3$ is shown in Fig. 1a. All diffraction peaks indexed to La-doped $NaTaO_3$ and confirms that high purity and good crystallinity is obtained in very short reaction times of 0.5–1.0 h at 900°C in a Na_2SO_4/K_2SO_4 flux. The refined unit cell parameters obtained from the PXRD pattern of all flux products are listed in Table 1, as well as that for the solid-state preparations with 0%, 1%, 2%, and 5% La doping. In general, the lattice parameters of all flux products were very similar to $\leq 0.005 \text{ \AA}$ and matched reasonably well with $\sim 2\%$ La doping, with the b parameter showing the most significant trend with doping. The parameters for 2% and 5% La-doping showed little change, with a

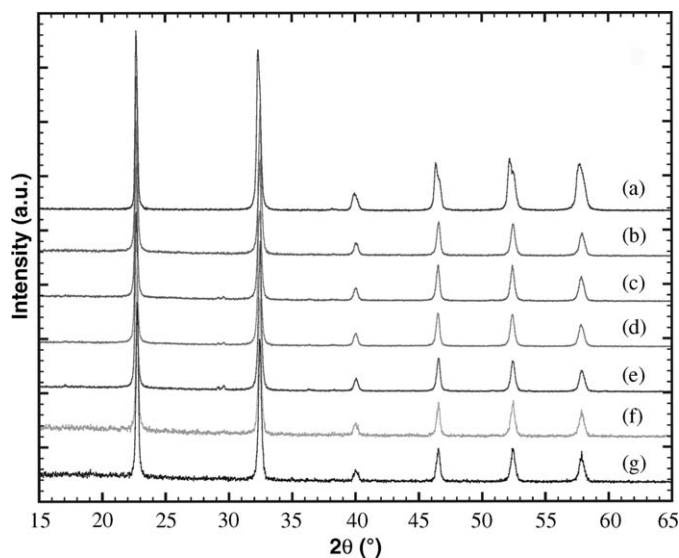


Fig. 1. Powder X-ray diffraction patterns of 2% La-doped NaTaO₃ synthesized by solid-state techniques (a) and using a Na₂SO₄/K₂SO₄ flux at 900 °C for 1 h for NaTaO₃:flux ratios of (b) 1:1, (c) 1:2 and (d) 1:3; and also for a reaction time of 0.5 h for NaTaO₃:flux ratios (e) 1:1, (f) 1:2 and (g) 1:3.

Table 1

Refined cell parameters^a for NaTaO₃ synthesized by the solid-state method for 0–5% La doping, and also by different flux conditions with 2% La doping^b

Sample name	<i>a</i> (Å)	<i>b</i> (Å)	<i>c</i> (Å)	Volume (Å ³)
NaTaO ₃ (0% La) ^c	5.5258(4)	7.8305(7)	5.5074(3)	238.30(3)
NaTaO ₃ (1% La) ^c	5.5255(5)	7.8290(7)	5.5103(3)	238.37(3)
NaTaO ₃ (2% La) ^c	5.5507(6)	7.8028(3)	5.5096(2)	238.63(3)
NaTaO ₃ (5% La) ^c	5.5412(5)	7.7977(4)	5.5081(3)	238.00(3)
NT1	5.5466(6)	7.7971(6)	5.5042(5)	238.04(4)
NT2	5.5467(7)	7.7996(7)	5.5052(5)	238.17(4)
NT3	5.5523(7)	7.7980(5)	5.5040(5)	238.31(4)
NT4	5.5485(7)	7.7982(6)	5.5044(5)	238.17(4)
NT5	5.5504(8)	7.7986(7)	5.5058(7)	238.32(5)
NT6	5.5481(6)	7.7969(6)	5.5040(5)	238.09(4)

^aUnit cell parameters were refined by a Le Bail fit [20] using the program FULLPROF [21].

^bLabeling for the reactions are as follows: for a reaction time of 1 h and NaTaO₃:flux ratios of 1:1 (NT1), 1:2 (NT2) and 1:3 (NT3) and a reaction time of 0.5 h and NaTaO₃:flux ratios of 1:1 (NT4), 1:2 (NT5) and 1:3 (NT6).

^cSynthesized using the reported solid-state synthesis method [10]: Na₂CO₃ (5% excess) La₂O₃ and Ta₂O₅ were finely ground together and heated to 1170 K for 1 h and to 1420 K for 10 h with an intermittent grinding.

minor unidentified impurity appearing in the PXRD pattern of the latter, indicating the saturation limit. Also, significant peak broadening was not observed for even the shortest reaction times and the largest amounts of flux, and was comparable to the solid-state preparation (i.e. compare Figs. 1a and b). Alternate synthetic preparations of non-doped NaTaO₃, including solvothermal [22], hydrothermal [13] and combustion syntheses [14], also do not exhibit

significant peak broadening at down to ~200 nm, but do give significant broadening at 5–20 nm. However, these preparations are for non-doped NaTaO₃ and have not yet been investigated for effects on the rate of photocatalytic hydrogen production.

In order to evaluate the particle sizes and morphologies, SEM analyses were performed on La-doped NaTaO₃ products synthesized by flux methods at 900 °C for 1.0 h, with a reactant:flux ratio of 1:4.8 and 1:2.4, shown in Figs. 2a and b, respectively. These images reveal aggregations of irregular block-like particles with dimensions of 100–500 nm as well as some smaller sizes. The smaller particles are obtained from the reaction with the larger amount of flux (1:4.8), as the particles in Fig. 2a were smaller by ×2–3 on average compared to those in Fig. 2b. For both reactions, the particles exhibited fairly rough surfaces and somewhat irregular block-shaped geometries, compared to the almost perfect cube-like particles reported from hydrothermal, solvothermal and combustion synthesis methods. The expression of rough surfaces, or nano-steps, on doped NaTaO₃ has previously been shown a key feature in its high photocatalytic activity [10]. An EDX analysis was performed (Supporting Information) and revealed detectable amounts of La, in addition to Na and Ta. Further, almost no K was found incorporated into the products, and which would have originated from cation exchange with the Na₂SO₄/K₂SO₄ flux.

The UV-Vis DRS were taken for each sample, shown in Fig. 3, and indicate both the size of the optical band gaps and the relative particle size trends of the products. The optical band gap (E_g) of non-doped bulk NaTaO₃ was previously found to be ~3.96 eV, while that of the La-doped (from 1% to 10%) NaTaO₃ series is a larger ~4.1 eV [10]. Using the formula E_g (eV) = 1240/ λ_g (nm), where λ_g (nm) is extrapolated from the linear rise in the absorption curve, the band gaps of the flux synthesized La-doped NaTaO₃ products are calculated to be in the range of ~4.13–4.17 eV. These results are consistent with La-doping into NaTaO₃, rather than non-doped NaTaO₃. Only very minimal quantum-size effects are observed, for example, between the products prepared via solid-state techniques (Fig. 3a; 4.13 eV) and the flux-synthesized products (Figs. 3b–g; 4.17 eV). However, the La-doped NaTaO₃ products with the smallest particle sizes would be expected to exhibit a significantly higher reflectance (i.e. highest scattering coefficients) [23,24]. Smaller particle sizes increases scattering and decreases light penetration, and which enhances the diffuse reflectance while decreasing the optical absorption. For samples prepared at 900 °C for 1 h, there is a clear trend towards increasing reflectance and therefore smaller particle sizes with increasing amounts of flux (Figs. 3b–d), in agreement with the SEM results above. The smallest diffuse reflectance, i.e. largest particle sizes, is observed for the products prepared by solid-state techniques (Fig. 3a). However, for the samples prepared in only 0.5 h at 900 °C (Figs. 3a–g) there is no significant difference among their diffuse reflectances, though they are larger

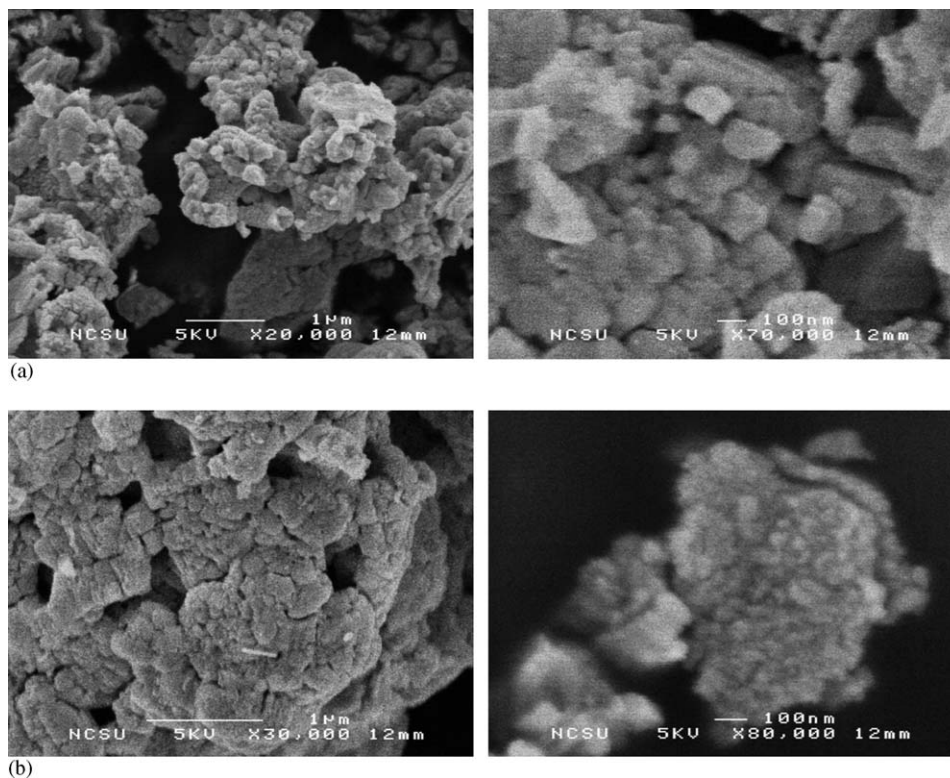


Fig. 2. Scanning electron microscopy images of La-doped NaTaO_3 synthesized via flux methods at 900°C and 1 h for NaTaO_3 :flux ratios of 1:4.8 (a) and 1:2.4 (b).

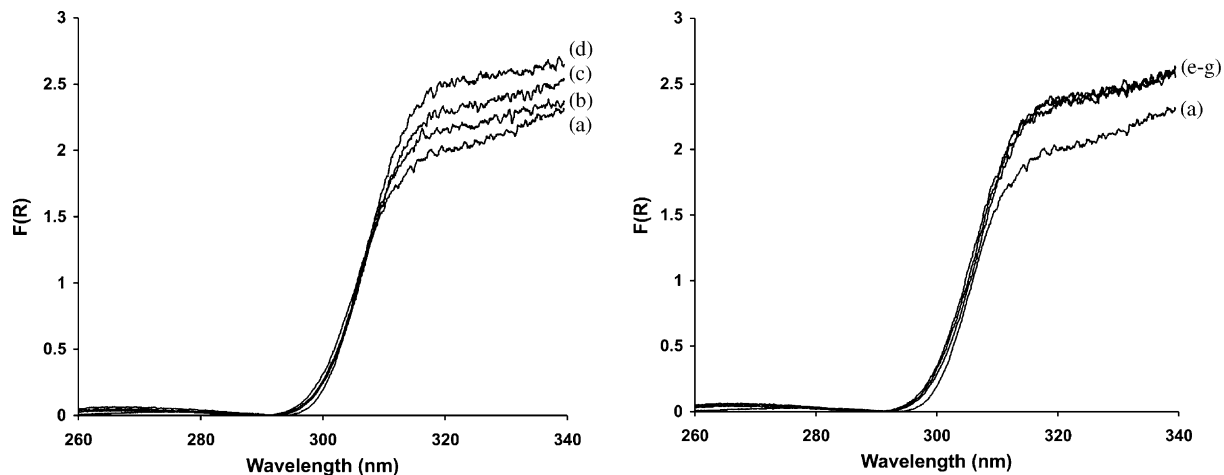


Fig. 3. Measured UV-Vis diffuse reflectance of 2% La-doped NaTaO_3 synthesized by solid-state techniques (a) and from flux reactions at 900°C for 1 h and NaTaO_3 :flux ratios of (b) 1:1, (c) 1:2 and (d) 1:3; and also for a reaction time of 0.5 h for NaTaO_3 :flux ratios (e) 1:1, (f) 1:2 and (g) 1:3.

than that found for the sample prepared by solid-state methods (Fig. 3a). For very small particles, such as in the nanometer size region, the diffuse reflectance reaches a maximum wherein the scattering is no longer expected to increase with decreasing particle size [23]. Further evidence for particle sizes and trends can be found in the photocatalysis testing (below).

The 2% La-doped NaTaO_3 solid, synthesized via solid-state methods, is known to be one of the most efficient photocatalysts, having up to a remarkable 56% quantum

efficiency in aqueous solutions. The accepted mechanism is that band-gap excitation produces a hole in the valence band that rapidly and irreversibly oxidizes surface methanol or water species, while the excited electron serves to reduce water at the Pt-cocatalyst surface sites. The stair-stepped surface features produced by La-doping into NaTaO_3 are postulated give rise to the very high efficiency, owing to the reduction and oxidation half-reactions being effectively separated by the fine surface features (edges/valleys). In order to test the effects of the flux synthesis

Table 2
Measured photocatalytic rates for NaTaO₃ (2% La-doped) prepared under varying flux conditions and a solid-state procedure

Sample (2% La-doped)	Synthetic conditions		Amount of H ₂ gas generated (mL h ⁻¹) ^a	Activity (μmol H ₂ h ⁻¹ g ⁻¹)
	NaTaO ₃ :flux ratio	Time (h)		
NaTaO ₃ std. ^b			2.5	560
NT1	1:1	1	5.0	1115
NT2	1:2	1	4.8	1070
NT3	1:3	1	3.5	780
NT4	1:1	0.5	4.2	940
NT5	1:2	0.5	3.7	825
NT5 ^c	1:2	0.5	4.0	895
NT6	1:3	0.5	2.4	535

^aTesting conditions: Outer irradiation 400 W high pressure Xe arc-lamp, 200 mg of 2% La-doped NaTaO₃ suspended in 20% aqueous methanol solution, and 1% Pt surface cocatalyst.

^bSynthesized using the reported solid-state synthesis method [10]: Na₂CO₃ (5% excess), La₂O₃, and Ta₂O₅ were finely ground together and heated to 1170 K for 1 h and to 1420 K for 10 h with an intermittent grinding.

^cTest performed using 2% Pt cocatalyst.

conditions and varying particle sizes on its photocatalytic activity, each sample was tested for photocatalytic H₂ production in an outer-irradiation quartz reaction cell in a 20% aqueous methanol solution. Methanol was employed in solution as a hole scavenger, thereby generating CO₂ as the oxidation product, so that the rate of reduction of H₂O to give H₂ formation is measured without the more difficult oxidation of H₂O to give O₂. The La-doped NaTaO₃ products were all found to exhibit very high photocatalytic activities, given in Table 2, with copious amounts of gas produced in each case. With increasing amounts of flux, i.e. smaller particle sizes, the photocatalytic rates decrease by about 30–40%. For example, for the products prepared at 900 °C and 1 h, the maximum observed rate of 1115 μmol H₂ h⁻¹ g⁻¹ decreases to 780 μmol H₂ h⁻¹ g⁻¹ on going from a 1:1 to 1:3 NaTaO₃:flux ratio, respectively. Also, the photocatalytic rates for the flux-synthesized products prepared in 0.5 h are ~70–85% to that for the products prepared in a longer reaction time of 1 h, confirming the trend towards decreasing photocatalytic rates with smaller particle sizes. A doubling of the amount of surface cocatalyst Pt from 1% to 2% in sample NT5, in order to compensate for its higher surface area, gave a relatively small 12.5% increase in the photocatalytic activity. However, nearly all measured photocatalytic rates for the flux-synthesized products were higher than that obtained by the solid-state method, at up to × 2 greater. Thus, the particle morphology and fine surface features that are produced during the flux synthesis of La-doped NaTaO₃, rather than the higher total surface areas, are the predominant factors leading to the enhanced photocatalytic rates.

4. Conclusions

Flux synthetic conditions, using a molten Na₂SO₄/K₂SO₄ mixture at 900 °C, can be used to prepare La-doped NaTaO₃ in high purity and homogeneity in much

shortened reaction times of 0.5–1.0 h compared to conventional solid-state techniques. The irregular block-shaped particles decrease in size from 500–100 nm with an increasing NaTaO₃:flux ratio (1:1, 1:2 to 1:3), as well as for the shorter reaction time of 0.5 h. The products show an optical band gap of ~4.13–4.17 eV and lattice constants consistent with ~2% La-doped NaTaO₃. Their photocatalytic activities in aqueous methanol solutions were 535–1115 μmol H₂ h⁻¹ g⁻¹, with the maximum rates for the largest particle sizes and the smallest amounts of flux used in their syntheses. These rates were up to × 2 greater than that for La-doped NaTaO₃ prepared by solid-state methods, demonstrating the utility of flux synthetic methods in photocatalysis research.

Acknowledgment

Support of this work is acknowledged from the Beckman Foundation through the Beckman Young Investigator Program (PM).

Supporting Information

An energy-dispersive X-ray analysis of a representative flux-synthesized product.

Appendix A. Supplementary materials

Supplementary data associated with this article can be found in the online version at doi:10.1016/j.jssc.2006.03.008.

References

- [1] K. Domen, J.N. Kondo, M. Hara, T. Takata, Bull. Chem. Soc. Jpn. 73 (2000) 1307.
- [2] H. Kato, A. Kudo, Catal. Today 78 (2003) 561–569.
- [3] A. Kudo, H. Kato, I. Tsuji, Chem. Lett. 33 (2004) 1534–1539.
- [4] C. Zhang, Y. Zhu, Chem. Mater. 17 (2005) 3537–3545.

- [5] J. Yoshimura, Y. Ebina, J. Kondo, K. Domen, A. Tanaka, *J. Phys. Chem.* 97 (1993) 1970–1973.
- [6] T. Takata, K. Shinohara, A. Tanaka, M. Hara, J.N. Kondo, K. Domen, *J. Photochem. Photobiol. A* 106 (1997) 45–49.
- [7] T. Takata, Y. Furumi, K. Shinohara, A. Tanaka, M. Hara, J.N. Kondo, K. Domen, *Chem. Mater.* 9 (1997) 1063–1064.
- [8] Y. Inoue, Y. Asai, K. Sato, *J. Chem. Soc. Faraday Trans.* 90 (1994) 797–802.
- [9] Y. Inoue, T. Kubokawa, K. Sato, *J. Chem. Soc. Chem. Commun.* (1990) 1298–1299.
- [10] H. Kato, K. Asakura, A. Kudo, *J. Am. Chem. Soc.* 125 (2003) 3082–3089.
- [11] A. Kudo, H. Kato, *Chem. Phys. Lett.* 331 (2000) 373–377.
- [12] A. Iwase, H. Kato, H. Okutomi, A. Kudo, *Chem. Lett.* 33 (2004) 1260–1261.
- [13] Y. He, Y. Zhu, N. Wu, *J. Solid State Chem.* 177 (2004) 3868–3872.
- [14] J. Xu, D. Xue, C. Yan, *Mater. Lett.* 59 (2005) 2920–2922.
- [15] D.B. Hedden, C.C. Torardi, W. Zegarski, *J. Solid State Chem.* 118 (1995) 419–421.
- [16] Y. Kana, X. Jina, P. Wanga, Y. Lia, Y. Chengb, D. Yan, *Mater. Res. Bull.* 38 (2003) 567.
- [17] T. Kimura, T. Yamaguchi, *J. Mater. Sci.* 17 (1982) 1863.
- [18] M. Granahan, M. Holmes, W.A. Schulze, R.E. Newnham, *J. Am. Ceram. Soc.* 64 (1982) C-68.
- [19] D.G. Porob, P.A. Maggard, *Mater. Res. Bull.* (2006), in press.
- [20] A. Le Bail, H. Duroy, J.L. Fourquet, *Mater. Res. Bull.* 23 (1988) 447–452.
- [21] J. Rodriguez-Carvajal, Fullprof 2k, Version 3.4 (November 2005), Laboratoire Leon, Brillouin (CEA/CNRS), CEA-Saclay, 91191 Gif-sur-Yvette Cedex, France.
- [22] Y. He, Y. Zhu, *Chem. Lett.* 33 (2004) 900–901.
- [23] M.G. Lagorio, *J. Chem. Edu.* 81 (11) (2004) 1607.
- [24] A.A. Christy, Y.-Z. Liang, C. Hui, O.M. Kvalheim, *Vib. Spectrosc.* 5 (1993) 233.